Ex vivo metabolic fingerprinting identifies biomarkers predictive of prostate cancer recurrence following radical prostatectomy

Running title: Metabolites in prostate cancer predict recurrence

Peder R. Braadland[1,2], Guro Giskeødegård[3], Elise Sandsmark[3], Helena Bertilsson[4,5], Leslie R. Euceda[3], Ailin F. Hansen[3], Ingrid J. Guldvik[1], Kirsten Selnæs[3], Helene H. Grytli[1], Betina Katz[6], Aud Svindland[2,6], Tone F. Bathen[3], Lars M. Eri[2,7], Ståle Nygård[8], Viktor Berge[7], Kristin A. Taskén[1,2], May-Britt Tessem[3]

[1] Department of Tumor Biology, Institute for Cancer Research, Oslo University Hospital, Oslo 0424, Norway.
[2] Institute of Clinical Medicine, Faculty of Medicine, University of Oslo, Oslo 0313, Norway
[3] Department of Circulation and Medical Imaging, Faculty of Medicine and Health Sciences, NTNU - Norwegian University of Science and Technology, Trondheim 7491, Norway
[4] St. Olavs Hospital, Trondheim University Hospital, Trondheim 7030, Norway
[5] Department of Cancer Research and Molecular Medicine, Faculty of Medicine, NTNU - Norwegian University of Science and Technology, Trondheim 7491, Norway
[6] Department of Pathology, Oslo University Hospital, Oslo 0424, Norway
[7] Department of Urology, Oslo University Hospital, Oslo 0424, Norway
[8] Bioinformatics Core Facility, Institute for Medical Informatics, Oslo University Hospital, Oslo 0424, Norway

Keywords: Biochemical recurrence; HR-MAS MRS; Magnetic Resonance Spectroscopy; Metabolomics; Metabolic fingerprinting; Prognostic biomarkers; Prostate cancer; Prostate cancer recurrence; Spermine; Citrate

Financial support: The Movember Foundation, the Norwegian Cancer Society, University of Oslo, Norwegian University of Science and Technology. St. Olavs Hospital and Oslo University Hospital

Corresponding authors: Kristin A. Taskén, May-Britt Tessem

Kristin A. Taskén, Institute for Cancer Research, Oslo University Hospital, P O Box 4953 Nydalen, NO-0424 Oslo, Norway, (0047) 22781878, k.a.tasken@medisin.uio.no.

May-Britt Tessem, Postboks 8905, MTFS, NTNU 7491 Trondheim, (0047) 73598836, may-britt.tessem@ntnu.no.

The authors declare no potential conflicts of interest.

Word count: 4053

Total number of figures and tables: 6

Abstract

Background

Robust biomarkers which identify prostate cancer patients with high risk of recurrence will improve personalized cancer care. In this study, we investigated whether tissue metabolites detectable by high-resolution magic angle spinning magnetic resonance spectroscopy (HR-MAS MRS) were associated with recurrence following radical prostatectomy.

Methods

We performed a retrospective *ex vivo* study using HR-MAS MRS on tissue samples from 110 radical prostatectomy specimens obtained from three different Norwegian cohorts collected between 2002-2010. At the time of analysis, 50 patients had experienced prostate cancer recurrence. Associations between metabolites, clinicopathological variables, and recurrence-free survival were evaluated using Cox proportional hazards regression modeling, Kaplan-Meier survival analyses and concordance index (C-index).

Results

High intratumoral spermine and citrate concentrations were associated with longer recurrence-free survival, whereas high (total-choline+creatine)/spermine (tChoCre/Spm) and higher (total-choline+creatine)/citrate (tChoCre/Cit) ratios were associated with shorter time to recurrence. Spermine concentration and tChoCre/Spm were independently associated with recurrence in multivariate Cox proportional hazards modeling after adjusting for clinically relevant risk factors (C-index: 0.769; HR: 0.72; P = 0.016, and C-index: 0.765; HR: 1.43; P = 0.014, respectively).

Conclusion

Spermine concentration and tChoCre/Spm ratio in prostatectomy specimens were independent prognostic markers of recurrence. These metabolites can be non-invasively measured *in vivo* and may thus offer predictive value to established preoperative risk assessment nomograms.

Introduction

Despite the curative intent of radical prostatectomy for localized prostate cancer, 15-30% of men who undergo resection develop biochemical recurrence (BCR) (Pound *et al*, 1999, Ward *et al*, 2003). Although BCR does not necessarily lead to lethal disease, 34% of men who experience BCR progress to develop metastases within eight years following radical prostatectomy (Pound *et al*, 1999). Novel markers capable of predicting recurrence are thus needed to identify patients eligible for treatment and active surveillance.

Current decision-making nomograms are commonly based on clinical staging, serum prostate-specific antigen (PSA), and histological findings on tissue biopsies (Canfield *et al*, 2014). Unfortunately, limitations to these parameters used in clinical practice lead to over-diagnosis of men with indolent disease, and conversely aggressive cancers are missed. Several promising molecular tests for predicting biochemical recurrence following radical prostatectomy are emerging, such as the genetic signature-based Prolaris assay (Bishoff *et al*, 2014), OncotypeDX Genomic Prostate Score (Cullen *et al*, 2015) and the Decipher genomic classifier (Erho *et al*, 2013). These tests require however invasive sampling by needle biopsies of significant cancer foci, which is challenging due to the multifocality and heterogeneity of prostate cancer (Canfield *et al*, 2014), and do not have the non-invasive potential of whole-prostate characterization, such as magnetic resonance (MR) imaging modalities which are appealing alternatives as prognostic tools.

MR spectroscopy (MRS) enables concurrent identification and quantification of several metabolites, which collectively constitute the metabolic fingerprint of a tissue sample (Kumar *et al*, 2016). In 2010, a retrospective *ex vivo* study displayed the potential of distinguishing non-recurrent from recurrent prostate cancers in a small cohort of patients

after RP using metabolite profiles obtained by *ex vivo* high-resolution magic angle spinning MRS (HR-MAS MRS) (Maxeiner *et al*, 2010). The paper received attention as the findings suggested a potential utility of MRS-based technology preoperatively (Sciarra, 2010). The potential clinical utility of this was further demonstrated with data from our group showing correlations between metabolites identified *ex vivo* and *in vivo* using HR-MAS MRS and MRSI, respectively (Selnaes *et al*, 2013). We also showed that low concentrations of spermine and citrate as well as a high (choline+creatine+polyamines)/citrate ratio were associated with high Gleason score using HR-MAS MRS (Giskeodegard *et al*, 2013). Recently, the number of polyamine-free voxels from *in vivo* MRS imaging (MRSI) was reported to be positively associated with biochemical recurrence following radical prostatectomy (Zakian *et al*, 2016).

In vivo MRSI has lower sensitivity and resolution than *ex vivo* MRS, and metabolites visible in *in vivo* prostate MRSI are usually limited to citrate, total-choline, creatine and polyamines. The low resolution causes overlapping peaks which hampers quantification of individual metabolites, and the lack of robust internal standards has warranted calculations of metabolite ratios. However, new developments in MRSI allow for absolute metabolite quantification (Weis *et al*, 2016), and faster and more automated protocols. Furthermore, implementation of higher magnetic field strengths and new pulse sequences can increase sensitivity (Lagemaat *et al*, 2016, Steinseifer *et al*, 2015). Thus, MRSI has the potential to play a future role in clinical practice to improve precision medicine.

In the current study, we identified prognostic metabolites predicting recurrence using *ex vivo* HR-MAS MRS on tissue samples from 110 patients treated with radical

prostatectomy. We show that metabolic profiling provides prognostic information independently of clinicopathological parameters, and discuss the possibility for *in vivo* use.

Materials and Methods

Patient selection

Patients (n=136) radically operated for prostate cancer between 2002 and 2010 at Oslo University Hospital, Oslo, Norway (OUS cohort, n=55) or at St. Olavs Hospital, Trondheim, Norway (NTNU1 cohort, n=39 and NTNU2 cohort, n=42) were retrospectively included in this study. Patients were excluded due to lack of follow-up data (n=5), lack of available tumor tissue (n=5), unsatisfactory HR-MAS MRS spectral quality (n=4) and due to administration of adjuvant and/or neoadjuvant therapy (n=12), leaving a total of 110 patients eligible for analysis. Recurrent prostate cancer was defined as biochemical recurrence (PSA ≥ 0.2 ng/mL with a subsequent rise). If PSA-measurements were missing, (n = 2 patients), time of recurrence was set to onset of salvage radiation therapy or salvage androgen deprivation therapy.

Ethical Approval of Studies and Informed Consent

The studies were approved by the Regional Committee for Medical and Health Research Ethics (REC) (2009/1028 and 2013/1713 REC South-East and 2009/1161 and 010-04 REC Central), and informed written consent was obtained from all included patients.

Sample collection

Samples were kindly provided by the “Registry and Biobank for Urological Diseases” (OUS cohort, n=55), MR biobank (NTNU1 cohort, n=39), and Biobank1, St Olavs Hospital (NTNU2 cohort, n=104). The tissue samples from the OUS cohort were collected at Oslo University Hospital immediately after prostatectomy by excising and fresh freezing tissue samples from

areas identified as tumor by a pathologist. The NTNU1 cohort (MR Biobank) consists of tissue biopsies from St. Olavs University Hospital taken within ~1-2 minutes after surgical removal of the prostate and immediately stored in liquid nitrogen (Hansen *et al*, 2016, Sandsmark *et al*, 2017). The biopsies (~10 mg) were aimed at cancer areas previously detected by transrectal ultrasound guided biopsies (TRUS) with more than 1mm tumor. The NTNU2 cohort (Biobank 1) was collected as 2-mm fresh-frozen prostate slices from the middle of the prostate, and tissue cores (~10 mg) were extracted based on clinical histopathology on the two adjacent tissue slices (Bertilsson *et al*, 2011). Further protocols for sample collection following radical prostatectomy are described in Supplementary Materials and Methods.

Ex vivo **HR-MAS MRS**

Ex vivo HR-MAS MRS metabolic fingerprinting was performed as previously described (Giskeodegard *et al*, 2013) using frozen, intact tissue samples (mean weight 12.5 mg, range 3.00-21.9 mg) on a Bruker Avance DRX600 (14.1T) spectrometer (Bruker Biospin, Germany) equipped with a $^{1}H/^{13}C$ HR-MAS probe. Absolute quantification of the MR spectra was performed using LCModel (Provencher, 1993, Hansen *et al*, 2016, Giskeodegard *et al*, 2013) and reported in nmol/mg wet weight. Total choline was calculated as the sum of choline, phosphocholine and glycerophosphocholine.

Pathology

Experimental procedures for pathological examination of the OUS cohort (AS and BK) following HR-MAS MRS spectral acquisition are described in Supplementary Materials and Methods. The pathological procedures on paraffin-sections (NTNU1 cohort) and cryo-sections (NTNU2 cohort) are described in (Sandsmark *et al*, 2017, Hansen *et al*, 2016) and

(Giskeodegard *et al*, 2013), respectively. In all three cohorts, percentages of cancer, benign (glandular) epithelium, and stromal tissue were reported for each sample.

Statistics

Linear mixed modeling (LMM) was applied to test each metabolite concentration or ratio as a function of recurrence status at 5 years while correcting for multiple samples per patient (R version 3.0.3, NLME package). Metabolite concentrations and ratios were Box-Cox transformed prior to analysis, and the Benjamini-Hochberg method (Benjamini and Hochberg, 1995) was used to adjust for multiple testing, giving false discovery rate-corrected *P*-values (Q-values, Q).

Recurrence was used as the end-point in survival analyses, with time to event calculated from date of radical prostatectomy to onset of recurrence. Cox proportional hazards modeling (R version 3.0.3, survival package) was performed on univariate and multivariate models to evaluate the association of metabolites with recurrence. Clinicopathological variables found to be significantly associated with recurrence in univariate models, were included as covariates in multivariate models. In all analyses, Gleason scores were categorized according to the ISUP (International Society of Urological Pathology) Grade Group system (Gordetsky and Epstein, 2016) after directly converting the reported Gleason scores as follows: Gleason score 6, 7a, 7b, 8 and 9 corresponds to Grade Group 1, 2, 3, 4 and 5, respectively. The predictive accuracies of the models were tested with the Harrell's concordance index (C-index) (Harrell *et al*, 1982). To compare models with different number of covariates and investigate overfitting, leave-one-out cross validation of C-indexes (LOOCV C-index) was performed. LOOCV C-index was performed in R v3.03 as follows: For each individual *i,* we first fit a Cox model to the survival data, leaving *i* out in the

estimation. The resulting coefficient estimates, β_{-i}, were then used together with individual *i*'s covariate values x_i, to obtain the linear predictor $\eta_i = \beta_{-i} x_i$ for each individual *i*. This was done successively for each individual, thus obtaining a vector of linear predictors $\eta=\eta_1, \eta_2,\ldots, \eta_n$, where *n* is the number of individuals. This vector η was then used as a single covariate in the Cox proportional hazard model in order to calculate the C-index, which we refer to as the *LOOCV C-index*.

Selection of metabolites to be modeled in survival analyses was based on *Q*-values from LMM and the possibility of measuring by *in vivo* MRSI in its current technological state. The metabolite concentrations and ratios were $\log_2$-transformed prior to Cox proportional hazards modeling to obtain scale-independent hazard ratios. For all survival analyses, one sample was randomly selected for inclusion where more than one tumor sample was present for a patient (applicable only for the NTNU2 cohort). To validate the Cox proportional hazard models, 1000 computations with random selections of samples from patients with multiple available samples were run.

Decision curve analyses were performed in R (version 3.0.3, DecisionCurve package) to evaluate the multivariate models at different threshold probabilities for recurrence within the five-year mark. Recurrence-free patients lacking five years of follow-up were excluded (n=4). One patient lacked only 15 days to reach five years of follow-up, but was included nonetheless, leaving a total of 106 patients for the analyses. A basic model containing pathological variables included in the Cox proportional hazards multivariate models, a full model with spermine or tChoCre/Spm, a "treat all" function (calculated from the basic model), and a "treat none" function were tested. Briefly, net benefit was evaluated in the threshold probability range of 0-40%, with bootstrapping (n=500).

198 The Kaplan Meier method was used to depict differences in recurrence-free survival
199 among patients harboring tumors with above or below median values of the metabolites of
200 interest, and the Mantel-Haenszel log rank test was used to evaluate the differences in the
201 distributions (R v3.03, survival package). To test the validity of the results from the OUS
202 cohort in the two other cohorts, the cut-off points yielding the lowest log rank *P*-values were
203 used (Budczies *et al*, 2012).

204 Student's t-tests and exact Mantel-Haenszel linear-by-linear association tests were
205 used to test for differences in distributions of clinicopathological demographics according to
206 recurrence, and Mann Whitney U tests were performed to test for metabolite levels in the
207 OUS and NTNU cohorts individually (all three tests were performed in SPSS v.21 (IBM,
208 Chicago, IL)). Spearman's rank correlation analyses were performed using R (R v3.03, Hmisc
209 package).

210 Partial least squares discriminant analysis (PLS-DA) was performed in MATLAB
211 (Mathworks, Natick, MA) and PLS-toolbox (Eigenvector Research, Manson, WA) to search for
212 systematic differences in metabolite concentrations between the cohorts. PLS-DA was
213 performed with leave-one-out cross validation using n=10% of the patients (n=11).
214 Permutation testing (n=1000) was performed to examine the significance of the resulting
215 model.

216

Results

Patient characteristics

Of the 110 patients eligible for analysis, recurrence was observed for 50 patients at the time of follow-up. The median follow-up time was 2366 days for patients without recurrence and 900 days for patients with recurrence. The recurrent group had a significantly higher proportion of patients with extraprostatic extension (pT3a), seminal vesicle invasion (≥pT3b), and had higher Gleason grades, whereas no significant differences in age, preoperative prostate-specific antigen (PSA) and surgical margin status were detected. All clinicopathological characteristics of the pooled cohort are presented in Table 1.

Metabolite concentrations in non-recurrent and recurrent prostate cancers

A total of 25 metabolites were quantified from the HR-MAS MRS spectra (Fig. 1 and Supplementary Table S1). The spermine concentration (the most predominant polyamine in the polyamine region (Giskeodegard *et al*, 2013)) was significantly lower in the recurrent compared to the non-recurrent group (P = 0.001, Q = 0.025), whereas citrate approached statistical significance towards a decrease after correcting for multiple testing (P = 0.007, Q = 0.063). Neither choline, total choline (not shown), nor creatine were significantly different between the groups.

The (total choline + creatine) / spermine (tChoCre/Spm) ratio was significantly higher in samples from patients who experienced recurrence within five-years of follow-up (P = 0.002, Q = 0.025). The (total choline + creatine) / citrate (tChoCre/Cit) ratio approached statistical significance towards separating the groups (P = 0.011, Q = 0.079) (Fig. 1B and

Supplementary Table S1). Additionally, spermine and citrate concentrations were found to be highly correlated (Spearman's rho = 0.79, $P < 0.001$) (Supplementary Fig. S1).

After stratifying patients based on median metabolite or ratio levels, patients with high levels of spermine and citrate had a longer recurrence-free survival than patients with low levels of these metabolites as shown in the Kaplan-Meier plots (Fig. 2). For metabolite ratios, low ratios were associated with longer recurrence-free survival.

Predictive accuracy of metabolites for prostate cancer recurrence

Candidate metabolites with translational potential for *in vivo* MRSI were evaluated in Cox proportional hazards univariate and multivariate modeling to investigate their association with recurrence-free survival. In univariate Cox analyses, higher spermine and citrate concentrations were associated with a decreased risk of recurrence, while higher choline concentration, as well as the tChoCre/Spm and tChoCre/Cit ratios, were associated with an increased risk of recurrence (Table 2). The spermine concentration and the tChoCre/Spm ratio were independently associated with recurrence-free survival in multivariate models after adjusting for variables found to be predictive of recurrence in univariate models (Grade Group, EPE, SVI) (spermine model and tChoCre/Spm model, Table 2). The calculated hazard ratios were in good compliance with the output from random sampling where more than one sample was available for a patient (Supplementary Fig. S2). The hazard ratio of citrate was statistically significant in the univariate Cox analysis, suggesting high citrate levels to be associated with lower risk of recurrence. However, citrate was not statistically significant in the multivariate Cox model (Supplementary Table S2). Similarly, although not statistically significant, creatine was associated with a lower risk of recurrence, while choline and tChoCre/Cit were associated with an increased risk of recurrence in multivariate models.

The spermine concentration and the tChoCre/Spm ratio reached univariate C-statistics (predictive accuracy) of 0.667 and 0.660, respectively, which were higher than that of seminal vesicle invasion, but not extraprostatic extension and Grade Group (Table 3). A basic clinicopathological model containing Grade Group (1-5), extraprostatic extension and seminal vesicle invasion reached a leave-one-out cross-validated C-index (LOOCV C-index) of 0.749. Adding spermine or tChoCre/Spm to the basic model increased the LOOCV C-index to 0.769 and 0.765, respectively, thus both provided additional predictive power over clinicopathological parameters alone.

Decision curve analyses visualize the net benefit of a model according to different threshold probabilities (i.e. chance of recurrence based on evaluated risk factors) at which patients or clinicians may consider performing additional prognostic tests (Vickers and Elkin, 2006). In this study, decision curve analyses revealed a positive net benefit of adding spermine to the basic clinicopathological model at decision threshold probabilities from 13-28% (Supplementary Fig. S3). For tChoCre/Spm, the net benefit was positive in the decision threshold range 14-20%.

Variability between the three pooled cohorts

As the three cohorts were pooled, we investigated the reproducibility across the cohorts. The clinicopathological characteristics of each cohort is presented in Supplementary Table S3. The histopathological composition of the tissue samples analyzed is shown in Supplementary Fig. S4. The distribution of cancer tissue was highest in the NTNU2 cohort (mean 62%), which had the highest distribution of Grade Group ≥4 samples**,** whereas tissue samples from the NTNU1 and OUS cohorts had less cancerous tissue (mean 38% and 35%, respectively), but higher stromal content (mean 40% and 57%, respectively). The amount of

benign tissue was non-significantly lower in recurrent than in non-recurrent samples from the NTNU1 cohort.

Bar charts and a PLS-DA score plot describing the metabolic differences between the three cohorts are shown in Supplementary Fig. S5. The median metabolite concentrations across the cohorts showed similar trends, although the median concentrations and size of interquartile ranges displayed inter-cohort variance. A PLS-DA model with three latent variables (LVs) showed significant differences in metabolite concentrations between the cohorts ($p<0.001$) with an average classification accuracy of 92% (sensitivity = 91.7%, specificity = 92.3%). The loadings revealed that the OUS cohort was systematically different from the other two cohorts in its levels of isoleucine, leucine, glycerophosphoethanolamine (GPE) and citrate. The separation of the NTNU1 cohort was characterized by its taurine, valine, glutamate and myo-inositol levels, whereas NTNU2 had differential glycerophosphocholine (GPC), glutamine and ethanolamine levels. The Spermine concentration did not contribute to the variance observed between the cohorts.

We tested the validity of results obtained in the OUS cohort, which was most balanced in terms of clinicopathology, in the NTNU1 and NTNU2 cohorts separately. The cut-off points for metabolite concentrations and ratios that best separated the recurrent and non-recurrent group in the OUS cohort, were applied to dichotomize the patient populations in the two other cohorts. Kaplan-Meier analyses showed good reproducibility for spermine and citrate, and fair reproducibility for tChoCre/Cit (Supplementary Fig. S6). The cut-off value for tChoCre/Spm could not significantly separate the groups in the NTNU1 and NTNU2 cohorts.

Associations of metabolites with clinicopathology

The Spermine and the citrate concentrations were negatively correlated with Grade Group and pT-stage, whereas tChoCre/Spm and tChoCre/Cit were positively correlated with Grade Group and pT-stage (Fig. 3 and Supplementary Fig. S7). Using the Grade Groups from the HR-MAS-analyzed tissue samples gave similar correlation coefficients as using diagnostic Grade Groups from the RP-specimens (results not shown). Citrate and tChoCre/Cit had higher correlations to Grade Group than spermine and tChoCre/Spm. Extraprostatic extension was negatively correlated with spermine and citrate concentrations, whereas a positive correlation was observed for tChoCre/Spm and tChoCre/Cit. Seminal vesicle invasion was more modestly associated with the four metabolites/metabolite ratios, and none of the metabolites correlated with patient age at operation. Of note, patient age, RP Grade Group and extraprostatic extension were all positively correlated.

Discussion

In this study, we demonstrate by *ex vivo* HR-MAS MRS that both the concentration of spermine and the tChoCre/Spm ratio in radical prostatectomy specimens are independent biomarkers of recurrence. A similar trend was found for citrate concentration. A combination of metabolite concentrations and standard clinicopathological parameters gave better accuracies towards predicting recurrence than clinicopathological parameters alone, although the relative increases in predictive accuracies were modest. Furthermore, decision curve analyses revealed a net benefit of adding metabolic fingerprinting to already established risk factors, with spermine granting the greatest overall improvement in net benefit. Thus, metabolic fingerprinting may serve as an adjunct predictive parameter to established decision-making nomograms.

Spermine and citrate concentrations were the metabolites that best correlated with recurrence within five years following prostatectomy. The relative levels, but not concentrations, of polyamines, therein spermine, have previously been shown to predict biochemical recurrence in prostate cancer (Maxeiner *et al*, 2010). In support of this, a recent *in vivo* MRSI study demonstrated that the number of voxels with undetectable levels of polyamines was associated with recurrence (Zakian *et al*, 2016). Furthermore, polyamine concentrations have been reported to be reduced in malignant compared to benign prostate tissue (van der Graaf *et al*, 2000), and further decreased from low to high Gleason score (Giskeodegard *et al*, 2013).

Like spermine, citrate concentrations are significantly lower in tumors with high compared to low Gleason score (Giskeodegard *et al*, 2013), likely due to loss of capacity to accumulate zinc during neoplasia and progression leading to increased inhibition of citrate

341 accumulation (Costello and Franklin, 1997, Bertilsson *et al*, 2012). Hence, both citrate and
342 spermine are markers for benign, glandular structures, and their levels are expected to drop
343 during dedifferentiation (Zakian *et al*, 2016). In support of previous reports (Giskeodegard *et*
344 *al*, 2013, Swanson *et al*, 2003), we observed that spermine and citrate concentrations were
345 significantly negatively correlated with Grade Group in radical prostatectomy specimens,
346 although the correlation for spermine was modest. Both metabolites are constituents of the
347 seminal fluid, and are most likely produced by luminal cells due to their positive association
348 with luminal space (Sandsmark *et al*, 2017, Lynch *et al*, 1994). The finding that spermine, but
349 not citrate, remains independently associated with recurrence in multivariate models, may
350 relate to spermine's lower adherence to Gleason grade. This indicates a tissue architecture-
351 independent association of spermine with prostate cancer aggressiveness.

352 Both Spermine oxidase (SMOX) and Spermidine/Spermine N1-acetyltransferase
353 (SAT1) are enzymes which catalyze reactions in the polyamine pathway, with reactive
354 oxygen species as byproducts (Goodwin *et al*, 2008, Huang *et al*, 2015). Interestingly, both
355 enzymes are believed to play a role in prostate cancer progression (Huang *et al*, 2015,
356 Goodwin *et al*, 2008). We have previously shown that when the tissue composition was
357 balanced between prostate cancer and normal tissue samples, a significant upregulation of
358 SAT1 and SMOX accompanied by decreased spermine levels, but without a significant
359 upregulation of spermine synthase (SMS) was measured in cancer samples (Tessem *et al*,
360 2016). This fits with a significant reduction in spermine concentration in prostate cancer
361 samples. These observations may explain the association of spermine with prostate cancer
362 recurrence. However, the polyamine pathway is complex and involved in multiple signaling
363 pathways in human cells (Pegg, 2009) and whether lower spermine levels relates to

dedifferentiation and loss of luminal characteristics of prostate tissue should be further investigated.

Aside from the proposed utility of post-operative *ex vivo* HR-MAS MRS to predict recurrence, *in vivo* MRSI sequences may easily be added to multiparametric MR imaging (mpMRI) protocols before treatment (Shukla-Dave *et al*, 2009, Shukla-Dave *et al*, 2012). Of the available mpMRI sequences, MRSI has primarily been applied in research settings due to its dependence on radiologist expertise on the field, prolonged overall scan time, and the associated costs (Loffroy *et al*, 2015). Implementation of standardized and faster MRSI protocols at higher magnetic field strengths, and computer-assisted spectral interpretation, may circumvent issues related to reproducibility of MRSI across institutions due to varied degree of radiologist training. This could, in turn, lower the overall costs of implementation of MRSI in the clinic. Importantly, studies have shown that the molecular information provided by MRSI may improve sensitivity towards detection and localization of clinically significant prostate cancers compared to MRI alone (Wefer *et al*, 2000, Barentsz *et al*, 2012, Weinreb *et al*, 2016).

As the current study was performed on radical prostatectomy specimens, the interpretation of the results is limited to a post-surgery setting where treatment decision-making is limited to adjuvant or salvage treatment modalities. Ultimately, due to the large clinical challenge of improving the sensitivity towards identifying high risk patients, as well as the specificity towards identifying truly indolent disease, the incremental value of adding MRSI protocols in the diagnostic setting should be investigated. Our study indicates that intratumoral metabolites may add value to clinically applied nomograms, and the translational potential from *ex vivo* HR-MAS MRS to *in vivo* MRSI has previously been

demonstrated through a positive correlation between preoperative MRSI and HR-MAS MRS data from spatially matched tissue samples (Selnaes *et al*, 2013). Furthermore, the prognostic value of spermine presented in this study is in line with a previous MRSI study performed preoperatively where the authors looked at the number of polyamine-free image voxels (Zakian *et al*, 2016)., indicating that spermine and possibly other polyamines may indeed predict risk for recurrence.

We hypothesize that MRSI may have a pre-surgical clinical applicability in detecting recurrent and aggressive characteristics in patients diagnosed with low and intermediate risk cancers. These patients may be offered radical treatment or adjuvant approaches such as radiation therapy and/or hormonal therapy (Tessem *et al*, 2016, Zapatero *et al*, 2015), as well as extended lymph node dissection (Gordetsky and Epstein, 2016). Furthermore, mpMRI-based approaches may detect tumors not discovered by biopsies (Hambrock *et al*, 2010), and confirmation of low- or very-low risk diagnoses may aid urologists in identifying patients eligible for active surveillance. Thus, future studies should be performed to establish the clinical utility of MRSI in prostate cancer precision medicine.

We recognize some limitations of this study. Firstly, the cohorts collectively contain a modest number of patients, and despite the fair reproducibility observed between the cohorts, validation in larger cohorts balanced in terms of clinicopathological parameters should be conducted. Secondly, the retrospective design may have introduced potential confounding that we have not been able to control for.

In summary, high concentration of spermine and low tChoCre/Spm ratio, determined by HR-MAS MRS of prostate cancer tissue, were associated with shorter time to recurrence

following radical prostatectomy. Both spermine and tChoCre/Spm are visible in *in vivo* MRSI, which opens for clinical translation of these candidate metabolic biomarkers.

Acknowledgements

We thank the patients who agreed to supply tissue and clinical follow-up data. We also thank the biobank “Registry and Biobank for Urological Diseases”, "Biobank 1", and the "MR biobank", and the people responsible for collecting and storing these data. We would like to thank pathologist Trond Viset (St. Olavs Hospital, Trondheim, Norway) for the grading of tissue in the NTNU1 and NTNU2 cohorts. Turid Follestad (NTNU, Trondheim, Norway) and Håkon Ramberg (OUS, Oslo, Norway) participated in counseling regarding statistical analyses, of which we are grateful. We acknowledge Alan J. Wright (Cancer Research UK, Cambridge, UK) for assistance with LCModel quantification of the MR spectra. We thank the Movember Foundation, the Norwegian Cancer Society, and Oslo University Hospital for funding the project. Finally, we thank Torill E. Sjøbakk (NTNU, Trondheim, Norway) and the Core Facility for MR (NTNU, Trondheim, Norway) for technical assistance and availability of experimental equipment.

References

Barentsz JO, Richenberg J, Clements R, Choyke P, Verma S, Villeirs G, Rouviere O, Logager V, Futterer JJ & European Society of Urogenital R (2012) ESUR prostate MR guidelines 2012. *Eur Radiol* **22**: 746-57, doi:10.1007/s00330-011-2377-y

Benjamini Y & Hochberg Y (1995) Controlling the False Discovery Rate - a Practical and Powerful Approach to Multiple Testing. *Journal of the Royal Statistical Society Series B-Methodological* **57**: 289-300, doi:

Bertilsson H, Angelsen A, Viset T, Skogseth H, Tessem MB & Halgunset J (2011) A new method to provide a fresh frozen prostate slice suitable for gene expression study and MR spectroscopy. *Prostate* **71**: 461-9, doi:10.1002/pros.21260

Bertilsson H, Tessem MB, Flatberg A, Viset T, Gribbestad I, Angelsen A & Halgunset J (2012) Changes in gene transcription underlying the aberrant citrate and choline metabolism in human prostate cancer samples. *Clin Cancer Res* **18**: 3261-9, doi:10.1158/1078-0432.CCR-11-2929

Bishoff JT, Freedland SJ, Gerber L, Tennstedt P, Reid J, Welbourn W, Graefen M, Sangale Z, Tikishvili E, Park J, Younus A, Gutin A, Lanchbury JS, Sauter G, Brawer M, Stone S & Schlomm T (2014) Prognostic utility of the cell cycle progression score generated from biopsy in men treated with prostatectomy. *J Urol* **192**: 409-14, doi:10.1016/j.juro.2014.02.003

Budczies J, Klauschen F, Sinn BV, Gyorffy B, Schmitt WD, Darb-Esfahani S & Denkert C (2012) Cutoff Finder: a comprehensive and straightforward Web application enabling rapid biomarker cutoff optimization. *PLoS One* **7**: e51862, doi:10.1371/journal.pone.0051862

Canfield SE, Kibel AS, Kemeter MJ, Febbo PG, Lawrence HJ & Moul JW (2014) A guide for clinicians in the evaluation of emerging molecular diagnostics for newly diagnosed prostate cancer. *Rev Urol* **16**: 172-80, doi:

Costello LC & Franklin RB (1997) Citrate metabolism of normal and malignant prostate epithelial cells. *Urology* **50**: 3-12, doi:10.1016/S0090-4295(97)00124-6

Cullen J, Rosner IL, Brand TC, Zhang N, Tsiatis AC, Moncur J, Ali A, Chen Y, Knezevic D, Maddala T, Lawrence HJ, Febbo PG, Srivastava S, Sesterhenn IA & Mcleod DG (2015) A Biopsy-based 17-gene Genomic Prostate Score Predicts Recurrence After Radical Prostatectomy and Adverse Surgical Pathology in a Racially Diverse Population of Men with Clinically Low- and Intermediate-risk Prostate Cancer. *Eur Urol* **68**: 123-31, doi:10.1016/j.eururo.2014.11.030

Erho N, Crisan A, Vergara IA, Mitra AP, Ghadessi M, Buerki C, Bergstralh EJ, Kollmeyer T, Fink S, Haddad Z, Zimmermann B, Sierocinski T, Ballman KV, Triche TJ, Black PC, Karnes RJ, Klee G, Davicioni E & Jenkins RB (2013) Discovery and validation of a prostate cancer genomic classifier that predicts early metastasis following radical prostatectomy. *PLoS One* **8**: e66855, doi:10.1371/journal.pone.0066855

Giskeodegard GF, Bertilsson H, Selnaes KM, Wright AJ, Bathen TF, Viset T, Halgunset J, Angelsen A, Gribbestad IS & Tessem MB (2013) Spermine and Citrate as Metabolic Biomarkers for Assessing Prostate Cancer Aggressiveness. *Plos One* **8**: e62375, doi:10.1371/journal.pone.0062375

Goodwin AC, Jadallah S, Toubaji A, Lecksell K, Hicks JL, Kowalski J, Bova GS, De Marzo AM, Netto GJ & Casero RA, Jr. (2008) Increased spermine oxidase expression in human prostate cancer and prostatic intraepithelial neoplasia tissues. *Prostate* **68**: 766-72, doi:10.1002/pros.20735

Gordetsky J & Epstein J (2016) Grading of prostatic adenocarcinoma: current state and prognostic implications. *Diagn Pathol* **11**: 25, doi:10.1186/s13000-016-0478-2

Hambrock T, Somford DM, Hoeks C, Bouwense SA, Huisman H, Yakar D, Van Oort IM, Witjes JA, Futterer JJ & Barentsz JO (2010) Magnetic resonance imaging guided prostate biopsy in men with repeat negative biopsies and increased prostate specific antigen. *J Urol* **183**: 520-7, doi:10.1016/j.juro.2009.10.022

Hansen AF, Sandsmark E, Rye MB, Wright AJ, Bertilsson H, Richardsen E, Viset T, Bofin AM, Angelsen A, Selnaes KM, Bathen TF & Tessem MB (2016) Presence of TMPRSS2-ERG is associated with alterations of the metabolic profile in human prostate cancer. *Oncotarget* **7**: 42071-85, doi:10.18632/oncotarget.9817

Harrell FE, Jr., Califf RM, Pryor DB, Lee KL & Rosati RA (1982) Evaluating the yield of medical tests. *JAMA* **247**: 2543-6, doi:

Huang W, Eickhoff JC, Mehraein-Ghomi F, Church DR, Wilding G & Basu HS (2015) Expression of spermidine/spermine N(1) -acetyl transferase (SSAT) in human prostate tissues is related to prostate cancer progression and metastasis. *Prostate* **75**: 1150-9, doi:10.1002/pros.22996

Kumar D, Gupta A & Nath K (2016) NMR-based metabolomics of prostate cancer: a protagonist in clinical diagnostics. *Expert Rev Mol Diagn* **16**: 651-61, doi:10.1586/14737159.2016.1164037

Lagemaat MW, Breukels V, Vos EK, Kerr AB, Van Uden MJ, Orzada S, Bitz AK, Maas MC & Scheenen TW (2016) (1)H MR spectroscopic imaging of the prostate at 7T using spectral-spatial pulses. *Magn Reson Med* **75**: 933-45, doi:10.1002/mrm.25569

Loffroy R, Chevallier O, Moulin M, Favelier S, Genson PY, Pottecher P, Crehange G, Cochet A & Cormier L (2015) Current role of multiparametric magnetic resonance imaging for prostate cancer. *Quant Imaging Med Surg* **5**: 754-64, doi:10.3978/j.issn.2223-4292.2015.10.08

Lynch MJ, Masters J, Pryor JP, Lindon JC, Spraul M, Foxall PJ & Nicholson JK (1994) Ultra high field NMR spectroscopic studies on human seminal fluid, seminal vesicle and prostatic secretions. *J Pharm Biomed Anal* **12**: 5-19, doi:

Maxeiner A, Adkins CB, Zhang Y, Taupitz M, Halpern EF, Mcdougal WS, Wu CL & Cheng LL (2010) Retrospective analysis of prostate cancer recurrence potential with tissue metabolomic profiles. *Prostate* **70**: 710-7, doi:10.1002/pros.21103

Pegg AE (2009) Mammalian polyamine metabolism and function. *IUBMB Life* **61**: 880-94, doi:10.1002/iub.230

Pound CR, Partin AW, Eisenberger MA, Chan DW, Pearson JD & Walsh PC (1999) Natural history of progression after PSA elevation following radical prostatectomy. *JAMA* **281**: 1591-7, doi:

Provencher SW (1993) Estimation of metabolite concentrations from localized in vivo proton NMR spectra. *Magn Reson Med* **30**: 672-9, doi:

Sandsmark E, Hansen AF, Selnaes KM, Bertilsson H, Bofin AM, Wright AJ, Viset T, Richardsen E, Drablos F, Bathen TF, Tessem MB & Rye MB (2017) A novel non-canonical Wnt signature for prostate cancer aggressiveness. *Oncotarget* **8**: 9572-9586, doi:10.18632/oncotarget.14161

Sciarra A (2010) Words of wisdom. Re: Retrospective analysis of prostate cancer recurrence potential with tissue metabolomic profiles. Maxeiner A, Adkins CB, Zhang Y, et al. Prostate 2010;70:710-7. *Eur Urol* **58**: 315, doi:

Selnaes KM, Gribbestad IS, Bertilsson H, Wright A, Angelsen A, Heerschap A & Tessem MB (2013) Spatially matched in vivo and ex vivo MR metabolic profiles of prostate cancer -- investigation of a correlation with Gleason score. *NMR Biomed* **26**: 600-6, doi:10.1002/nbm.2901

Shukla-Dave A, Hricak H, Akin O, Yu C, Zakian KL, Udo K, Scardino PT, Eastham J & Kattan MW (2012) Preoperative nomograms incorporating magnetic resonance imaging and spectroscopy for prediction of insignificant prostate cancer. *BJU Int* **109**: 1315-22, doi:10.1111/j.1464-410X.2011.10612.x

Shukla-Dave A, Hricak H, Ishill N, Moskowitz CS, Drobnjak M, Reuter VE, Zakian KL, Scardino PT & Cordon-Cardo C (2009) Prediction of prostate cancer recurrence using magnetic resonance imaging and molecular profiles. *Clin Cancer Res* **15**: 3842-9, doi:10.1158/1078-0432.CCR-08-2453

Steinseifer IK, Van Asten JJ, Weiland E, Scheenen TW, Maas MC & Heerschap A (2015) Improved volume selective (1) H MR spectroscopic imaging of the prostate with gradient offset independent adiabaticity pulses at 3 tesla. *Magn Reson Med* **74**: 915-24, doi:10.1002/mrm.25476

Swanson MG, Vigneron DB, Tabatabai ZL, Males RG, Schmitt L, Carroll PR, James JK, Hurd RE & Kurhanewicz J (2003) Proton HR-MAS spectroscopy and quantitative pathologic analysis of MRI/3D-MRSI-targeted postsurgical prostate tissues. *Magn Reson Med* **50**: 944-54, doi:10.1002/mrm.10614

Tessem MB, Bertilsson H, Angelsen A, Bathen TF, Drablos F & Rye MB (2016) A Balanced Tissue Composition Reveals New Metabolic and Gene Expression Markers in Prostate Cancer. *PLoS One* **11**: e0153727, doi:10.1371/journal.pone.0153727

Van Der Graaf M, Schipper RG, Oosterhof GO, Schalken JA, Verhofstad AA & Heerschap A (2000) Proton MR spectroscopy of prostatic tissue focused on the detection of spermine, a possible biomarker of malignant behavior in prostate cancer. *MAGMA* **10**: 153-9, doi:

Vickers AJ & Elkin EB (2006) Decision curve analysis: a novel method for evaluating prediction models. *Med Decis Making* **26**: 565-74, doi:10.1177/0272989X06295361

Ward JF, Blute ML, Slezak J, Bergstralh EJ & Zincke H (2003) The long-term clinical impact of biochemical recurrence of prostate cancer 5 or more years after radical prostatectomy. *J Urol* **170**: 1872-6, doi:10.1097/01.ju.0000091876.13656.2e

Wefer AE, Hricak H, Vigneron DB, Coakley FV, Lu Y, Wefer J, Mueller-Lisse U, Carroll PR & Kurhanewicz J (2000) Sextant localization of prostate cancer: comparison of sextant biopsy, magnetic resonance imaging and magnetic resonance spectroscopic imaging with step section histology. *J Urol* **164**: 400-4, doi:

Weinreb JC, Barentsz JO, Choyke PL, Cornud F, Haider MA, Macura KJ, Margolis D, Schnall MD, Shtern F, Tempany CM, Thoeny HC & Verma S (2016) PI-RADS Prostate Imaging - Reporting and Data System: 2015, Version 2. *Eur Urol* **69**: 16-40, doi:10.1016/j.eururo.2015.08.052

Weis J, Von Below C, Tolf A, Ortiz-Nieto F, Wassberg C, Haggman M, Ladjevardi S & Ahlstrom H (2016) Quantification of metabolite concentrations in benign and malignant prostate tissues using 3D proton MR spectroscopic imaging. *J Magn Reson Imaging*, doi:10.1002/jmri.25443

Zakian KL, Hatfield W, Aras O, Cao K, Yakar D, Goldman DA, Moskowitz CS, Shukla-Dave A, Tehrani YM, Fine S, Eastham J & Hricak H (2016) Prostate MRSI Predicts Outcome in Radical Prostatectomy Patients. *Magn Reson Imaging* **34**: 674-81, doi:10.1016/j.mri.2016.01.003

Zapatero A, Guerrero A, Maldonado X, Alvarez A, Gonzalez San Segundo C, Cabeza Rodriguez MA, Macias V, Pedro Olive A, Casas F, Boladeras A, De Vidales CM, Vazquez De La Torre ML, Villa S, Perez De La Haza A & Calvo FA (2015) High-dose radiotherapy with short-term or long-term androgen deprivation in localised prostate cancer (DART01/05 GICOR): a randomised, controlled, phase 3 trial. *Lancet Oncol* **16**: 320-7, doi:10.1016/S1470-2045(15)70045-8

Titles and legends to figures

Fig. 1. Metabolite levels in non-recurrent and recurrent prostate cancers at the five-year mark. A. Average HR-MAS MRS spectra from tumors from non-recurrent (black) and recurrent (red) prostate cancer groups in the NTNU1 cohort. Magnifications of the polyamine (containing spermine and putrescine) and citrate regions are shown. **B.** Quantified peak integrals of spermine, citrate, choline and creatine (nmol/mg), and tChoCre/Spm and tChoCre/Cit ratios in the groups from all samples in all included cases from the three cohorts are shown as beeswarm plots (n=158). The thin horizontal lines make out the 25% and 75% quartiles, and the median value is shown as thick black horizontal lines. Statistical significance was calculated by LMM to account for multiple samples per patient (*: $P < 0.05$, **: $Q < 0.05$). Abbreviations: Ala = alanine; Cho = choline; Cit = citrate; Cre = creatine; Gln = glutamine; Glu = glutamate; Gly = glycine; Lac = lactate; Myo-ino = myo-inositol; NS = non-significant; PA = polyamines; PCho/GPC = phosphocholine and glycerophosphocholine peaks; *Sc*-ino = *scyllo*-inositol; Spm = spermine; Succ = succinate; Tau = taurine; tCho = total choline.

Fig. 2. **Kaplan-Meier plots.** Recurrence-free proportions plotted against time to first report of recurrence for spermine (**A**), citrate (**B**), tChoCre/Spm (**C**), and tChoCre/Cit (**D**) dichotomized to above and below median concentrations. Mantel-Haenszel log rank test was used to test for the null hypothesis of equal survival distributions (*P*-value indented). Abbreviations: tChoCre/Cit = (total-choline+creatine)/citrate.; tChoCre/Spm = (total-choline+creatine)/spermine.

Fig. 3. Correlation heatmap. Correlations between metabolites and clinicopathological factors. The Spearman correlation coefficients are shown inside the boxes (large font), with corresponding *P*-values below. The color scale indicates the sign of the correlation coefficients and the degree of correlation, where blue indicates negative correlation, white no correlation, and red positive correlation.

Table 1: Clinical and pathological characteristics of included patients from the pooled cohort.

	No recurrence (%)	Recurrence (%)	*P* -value
N	60	50	
Follow-up			
Median (IQR), d	2366 (455)	900 (1148)	
Age			
Mean ± SD, yr	61.7 ± 6	62.5 ± 5	0.42[a]
Preoperative PSA			
Mean ± SD, ng/ml	9.4 ± 5.8	10.3 ± 5.1	0.44[a]
Grade group (RP)			
1	4 (7)	5 (10)	
2	39 (65)	14 (28)	
3	15 (25)	17 (34)	<0.001[b]
4	2 (3)	7 (14)	
5	0 (0)	7 (14)	
EPE	9 (15)	31 (62)	<0.001[b]
SVI	4 (7)	12 (24)	0.014[b]
PSM	15 (25)	21 (42)	0.12[b]
PCa-specific death	0	3 (6)	

Abbreviations: EPE = extraprostatic extension; IQR = interquartile range; PSA = prostate-specific antigen; PSM = positive surgical margins; RP = radical prostatectomy; SVI = seminal vesicle invasion, PCa = prostate cancer.

[a]: Student's t-test;

[b]: Exact Mantel-Haenszel linear-by-linear association chi-squared test.

Table 2: Univariate and multivariate Cox proportional hazard ratios for metabolites and metabolite ratios and prostate cancer recurrence following radical prostatectomy.

	Univariate analysis		Multivariate analysis		Multivariate analysis	
			Spermine model		tChoCre/Spm model	
Variable	**HR (95% CI)**	***P*- value**	**HR (95% CI)**	***P*- value**	**HR (95% CI)**	***P*- value**
Spermine (log_2)	0.63 (0.50-0.80)	<0.001	0.72 (0.55-0.94)	0.016		
tChoCre/Spm (log_2)	1.55 (1.23-1.96)	<0.001			1.43 (1.08-1.91)	0.014
Citrate (log_2)	0.67 (0.51-0.86)	0.002				
tChoCre/Cit (log_2)	1.38 (1.11-1.71)	0.004				
Choline (log_2)	1.59 (1.05-2.39)	0.028				
Creatine (log_2)	0.75 (0.48-1.19)	0.22				
Age (continuous)	1.02 (0.97-1.07)	0.42				
Preoperative PSA	1.02 (0.98-1.07)	0.329				
Grade group (RP)						
1	Reference		Reference		Reference	
2	0.38 (0.14-1.05)	0.062	0.55 (0.18-1.70)	0.30	0.53 (0.17-1.65)	0.27
3	0.92 (0.34-2.51)	0.87	0.83 (0.28-2.44)	0.74	0.73 (0.24-2.23)	0.59
4	2.12 (0.67-6.71)	0.20	2.73 (0.81-9.18)	0.11	2.58 (0.76-8.72)	0.13
5	3.01 (0.95-9.56)	0.061	2.04 (0.61-6.85)	0.25	2.00 (0.60-6.71)	0.26
EPE	4.65 (2.61-8.27)	<0.001	3.03 (1.54-5.96)	0.0013	2.98 (1.51-5.89)	0.0017
SVI	3.39 (1.76-6.54)	<0.001	1.02 (0.46-2.72)	0.95	1.06 (0.49-2.31)	0.87
SM	1.67 (0.95-2.94)	0.074				

Abbreviations: CI = confidence interval; EPE = extraprostatic extension; RP = radical prostatectomy; SVI = seminal vesicle invasion; PSM = positive surgical margins; tChoCre/Cit = (total-choline+creatine)/citrate; tChoCre/Spm = (total-choline+creatine)/spermine.

Table 3: Concordance index (C-index) for univariate and multivariate models including spermine and the tChoCre/Spm metabolite ratio.

	Univariate analysis		Multivariate analysis		
Variable	**C-index**		**C-index**	**LOOCV C-index[a]**	**ΔC-index**
Spermine (log_2)	0.667	Full model	0.769	0.769	0.020
tChoCre/Spm (log_2)	0.660		0.765	0.765	0.016
Grade Group (RP)	0.694	Basic model	0.749	0.749	
EPE	0.697				
SVI	0.595				

Abbreviations: C-index = concordance index; EPE = extraprostatic extension; SVI = seminal vesicle invasion; tChoCre/Spm = (total-choline+creatine)/spermine; RP = radical prostatectomy. Grade group categorized 1-5. Full model refers to models containing metabolites on top of the basic model, whereas basic model refers to the pathological model without added metabolites.

[a] : Leave-one-out cross validated (LOOCV) C-indexes were used to calculate the change in C-index upon adding either spermine or tChoCre/Spm to the basic model (ΔC-index).

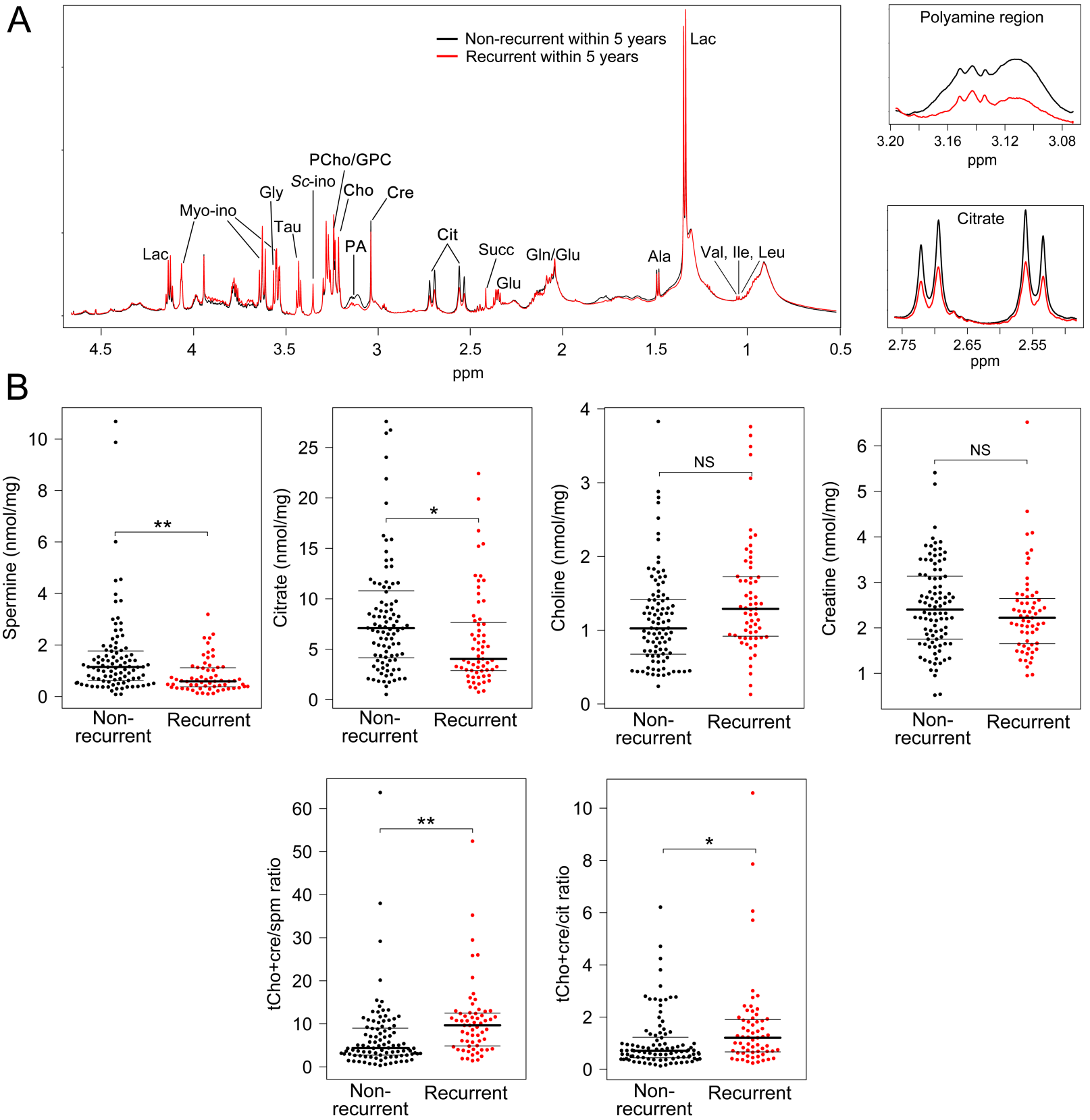
A
Non-recurrent within 5 years
Recurrent within 5 years
Lac
PCho/GPC
Sc-ino
Gly
Cho
Cre
Myo-ino
Tau
PA
Cit
Succ
Gln/Glu
Glu
Ala
Val, Ile, Leu
4.5
4
3.5
3
2.5
2
1.5
1
0.5
ppm
Polyamine region
3.20
3.16
3.12
3.08
ppm
Citrate
2.75
2.65
2.55
ppm
B
Spermine (nmol/mg)
**
Citrate (nmol/mg)
*
Choline (nmol/mg)
NS
Creatine (nmol/mg)
NS
tCho+cre/spm ratio
**
tCho+cre/cit ratio
*
Non-recurrent
Recurrent

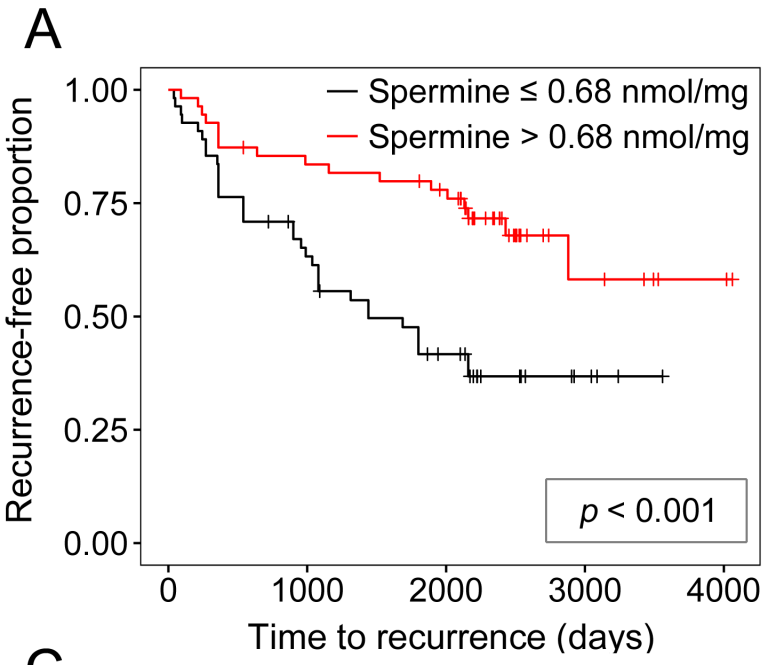
A
Spermine ≤ 0.68 nmol/mg
Spermine > 0.68 nmol/mg
p < 0.001
Recurrence-free proportion
1.00
0.75
0.50
0.25
0.00
0
1000
2000
3000
4000
Time to recurrence (days)

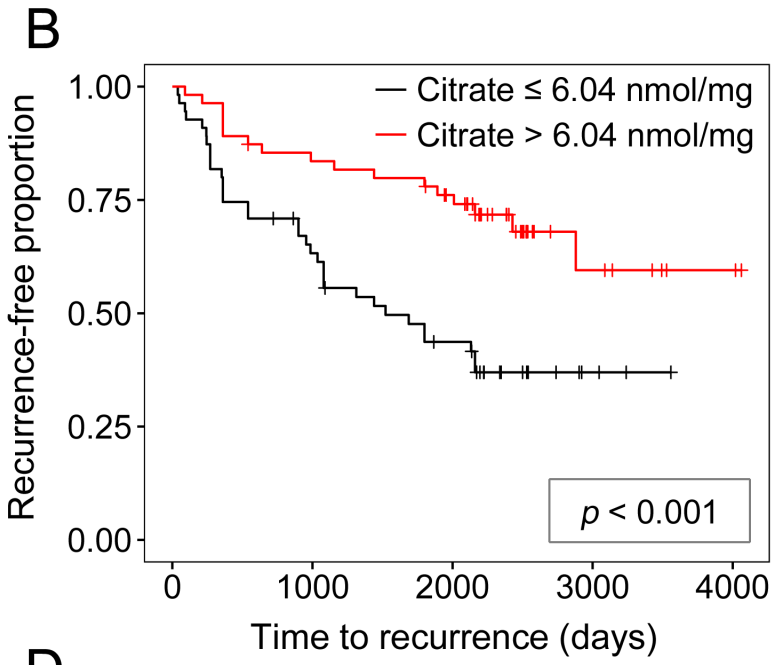
B
Citrate ≤ 6.04 nmol/mg
Citrate > 6.04 nmol/mg
p < 0.001
Recurrence-free proportion
1.00
0.75
0.50
0.25
0.00
0
1000
2000
3000
4000
Time to recurrence (days)

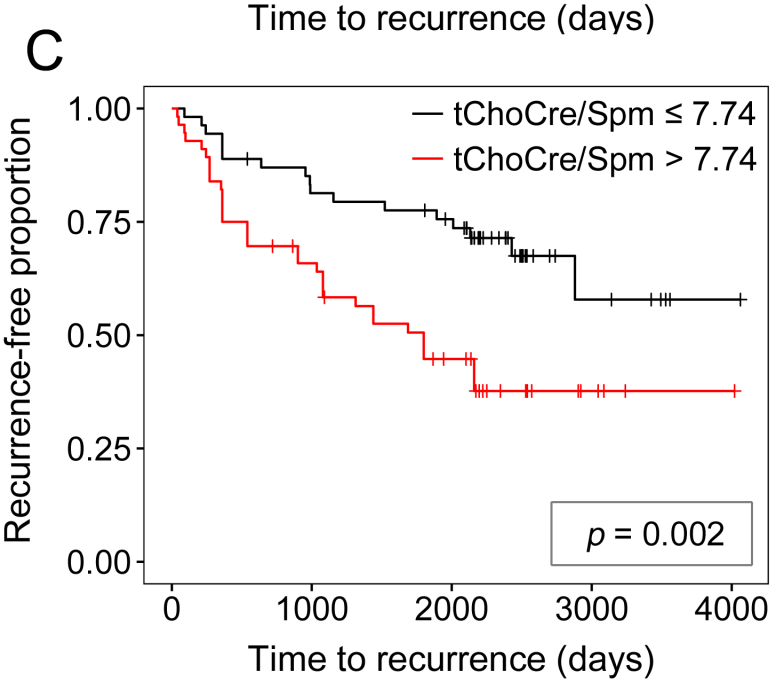
C
tChoCre/Spm ≤ 7.74
tChoCre/Spm > 7.74
p = 0.002
Recurrence-free proportion
1.00
0.75
0.50
0.25
0.00
0
1000
2000
3000
4000
Time to recurrence (days)

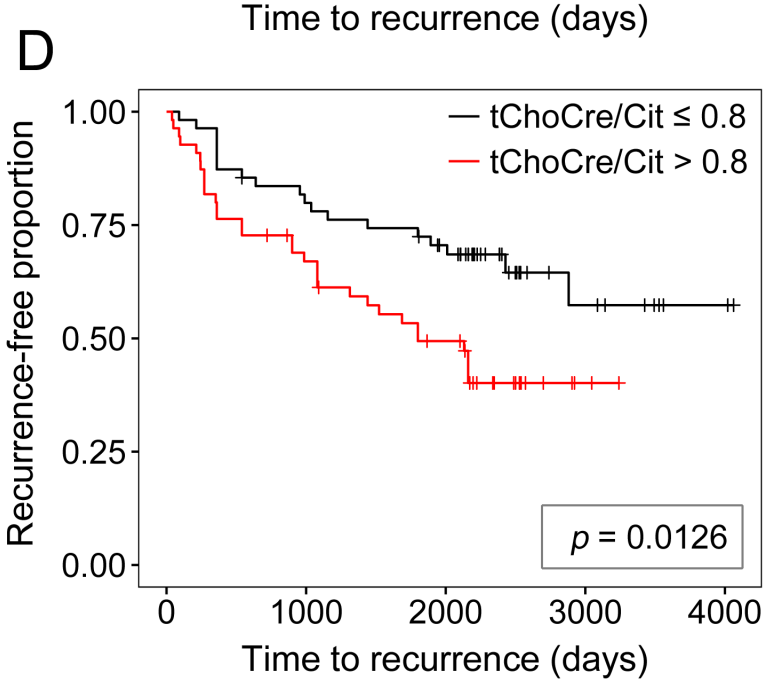
D
tChoCre/Cit ≤ 0.8
tChoCre/Cit > 0.8
p = 0.0126
Recurrence-free proportion
1.00
0.75
0.50
0.25
0.00
0
1000
2000
3000
4000
Time to recurrence (days)

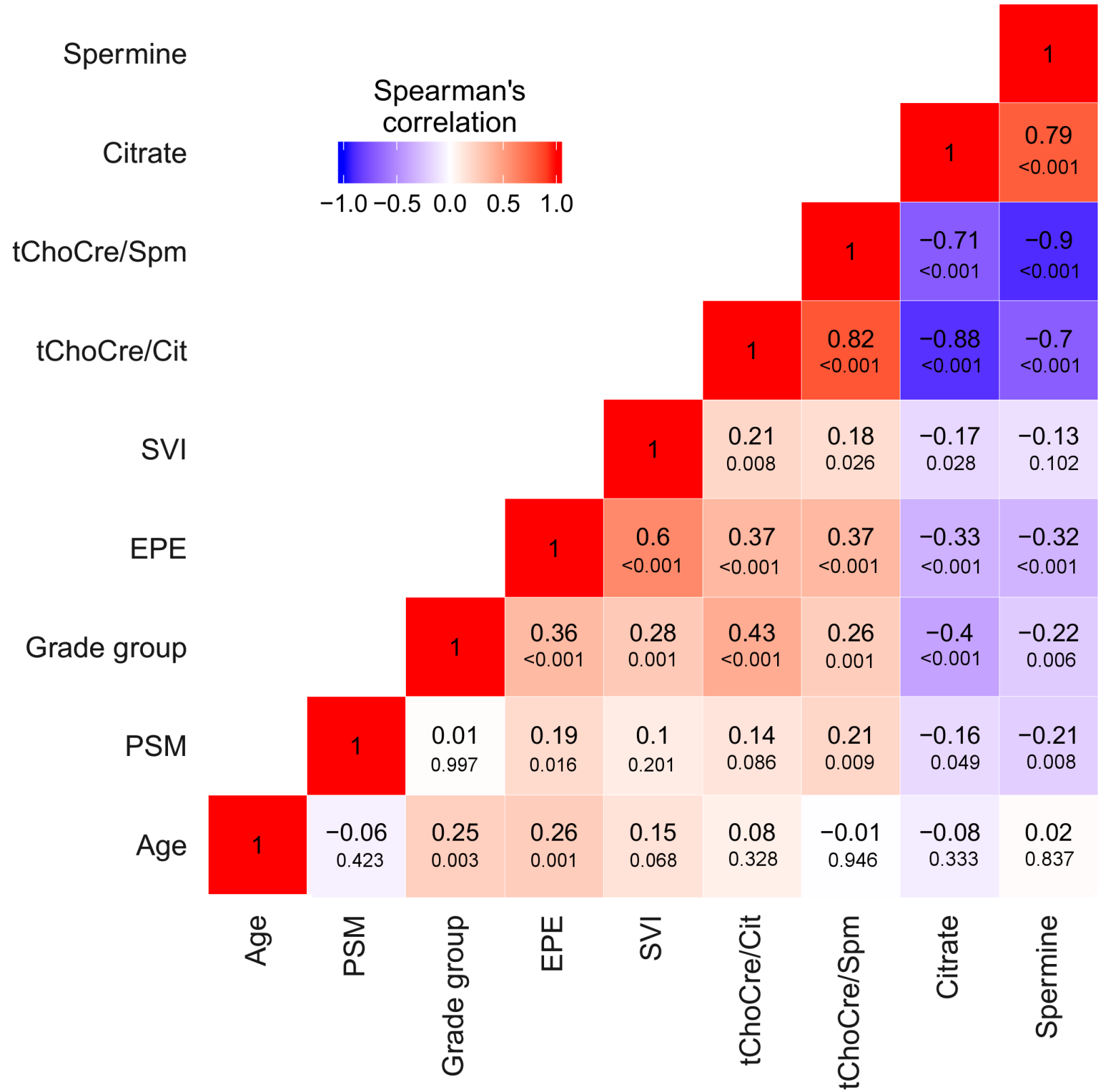
Spermine
Citrate
tChoCre/Spm
tChoCre/Cit
SVI
EPE
Grade group
PSM
Age
Spearman's correlation
−1.0 −0.5 0.0 0.5 1.0
1
1 0.79 <0.001
1 −0.71 <0.001 −0.9 <0.001
1 0.82 <0.001 −0.88 <0.001 −0.7 <0.001
1 0.21 0.008 0.18 0.026 −0.17 0.028 −0.13 0.102
1 0.6 <0.001 0.37 <0.001 0.37 <0.001 −0.33 <0.001 −0.32 <0.001
1 0.36 <0.001 0.28 0.001 0.43 <0.001 0.26 0.001 −0.4 <0.001 −0.22 0.006
1 0.01 0.997 0.19 0.016 0.1 0.201 0.14 0.086 0.21 0.009 −0.16 0.049 −0.21 0.008
1 −0.06 0.423 0.25 0.003 0.26 0.001 0.15 0.068 0.08 0.328 −0.01 0.946 −0.08 0.333 0.02 0.837
Age
PSM
Grade group
EPE
SVI
tChoCre/Cit
tChoCre/Spm
Citrate
Spermine